# Dramatically increasing chance of extremely hot summers since the 2003 European heatwave

Nikolaos Christidis*, Gareth S. Jones and Peter A. Stott

**Socio-economic stress from the unequivocal warming of the global climate system[1] could be mostly felt by societies through weather and climate extremes[2]. The vulnerability of European citizens was made evident during the summer heatwave of 2003 (refs 3,4) when the heat-related death toll ran into tens of thousands[5]. Human influence at least doubled the chances of the event according to the first formal event attribution study[6], which also made the ominous forecast that severe heatwaves could become commonplace by the 2040s. Here we investigate how the likelihood of having another extremely hot summer in one of the worst affected parts of Europe has changed ten years after the original study was published, given an observed summer temperature increase of 0.81 K since then. Our analysis benefits from the availability of new observations and data from several new models. Using a previously employed temperature threshold to define extremely hot summers, we find that events that would occur twice a century in the early 2000s are now expected to occur twice a decade. For the more extreme threshold observed in 2003, the return time reduces from thousands of years in the late twentieth century to about a hundred years in little over a decade.**

Despite the slowdown in the global mean temperature increase since the late 1990s (refs 7–9), hot temperature extremes have continued to warm on both global and regional scales[10,11]. Severe heatwaves in the past decade such as the ones in Moscow in 2010 (refs 12,13), Texas in 2011 (ref. 14) and the Australian 'angry summer' of 2012–2013[15] were characterized by long duration, large spatial extent and catastrophic impacts. Research on event attribution aims to identify the drivers of such extreme events and determine how possible causes such as human influence on the climate might have altered their odds[16–18]. In this paper we revisit the first study of this kind[6] that investigated the 2003 European heatwave and carry out a new analysis that is now extended to the present day. As in the original study, we concentrate on summer temperatures (average over June–August) in the land area bounded by 10° W–40° E and 30°–50° N, which, among a number of pre-defined climatic regions[19], was mostly affected by the 2003 heatwave. The use of a pre-defined region helps minimize selection bias. The selected area largely includes the countries where heat-related mortality peaked (France, Germany and Italy), but is more extensive.

Summer temperature time series constructed with the best estimate of the CRUTEM4 observational data set[20] show that the 2003 record was subsequently broken in 2012 (Fig. 1). Although a hot summer in the region cannot be directly linked to heatwave damage (for example, heatwave impacts in 2012 were less notable than in 2003), as records are being broken in a warming climate, hotter summers are generally expected to be associated with more severe impacts. Our analysis examines how the likelihood of very warm summers in the region has changed between the time the actual event occurred, using estimates of the forced climatic change in the 1990s, and the present day, using the more recent decade of 2003–2012. Interestingly, the recent decade is 0.81 K warmer than the 1990s (Fig. 1), indicating a shift of the summer temperature distribution towards higher values, which would increase the chances of new record-breaking temperatures.

We also employ modelled temperature estimates from simulations of the climate with all historical external climatic forcings (ALL) and with natural forcings alone (NAT) produced with seven models that contributed data to the archive of the World Climate Research Programme's Coupled Model Intercomparison Project phase 5 (CMIP5; ref. 21). Each model provides at least 3 simulations for each experiment, as well as more than 500 years of a control simulation of the unforced climate. We use all models that provide NAT simulations extended to year 2012 and so end up with 43 ALL simulations, 33 NAT simulations and over 6,000 modelled years of the control climate (Supplementary Information). The temperature increase in recent decades is evident only in simulations that include human influence on the climate (Fig. 1).

We next employ optimal fingerprinting[22], a generalized multivariate regression methodology that has been widely used in detection and attribution studies of climate change[1,6,23]. We partition observed changes in the regional summer temperatures since the early twentieth century between the contributions of anthropogenic and natural forcings and internal variability (Methods). Optimal fingerprinting scales modelled time series of the decadal mean summer temperature in the reference region with and without anthropogenic forcings to bring their linear combination in best agreement with the CRUTEM4 observations. If the scaling factor of the response to specific forcings (anthropogenic or natural) is not consistent with zero, then the effect of these forcings is deemed detectable in the observations. We carry out two analyses: the first ends in decade 1990–1999, which gives the climate response to external forcings near the time of the 2003 heatwave (same as in previous work[6]); the second ends in decade 2003–2012 and provides the response in the present day. The use of a recent decade to represent the current climate is a common limitation in attribution studies[6,24] that may introduce a low bias on estimates of the likelihood of extreme events. Using a decade centred on the current year as an alternative would be feasible only for model projections but not observational data. Using a multi-model ensemble mean[23] to construct the temperature time series employed in the analyses can potentially minimize the effect of individual model biases. The effect of internal variability is derived from control simulations with the seven models and power spectra assessments indicate that the modelled variability is consistent with the observations[24].
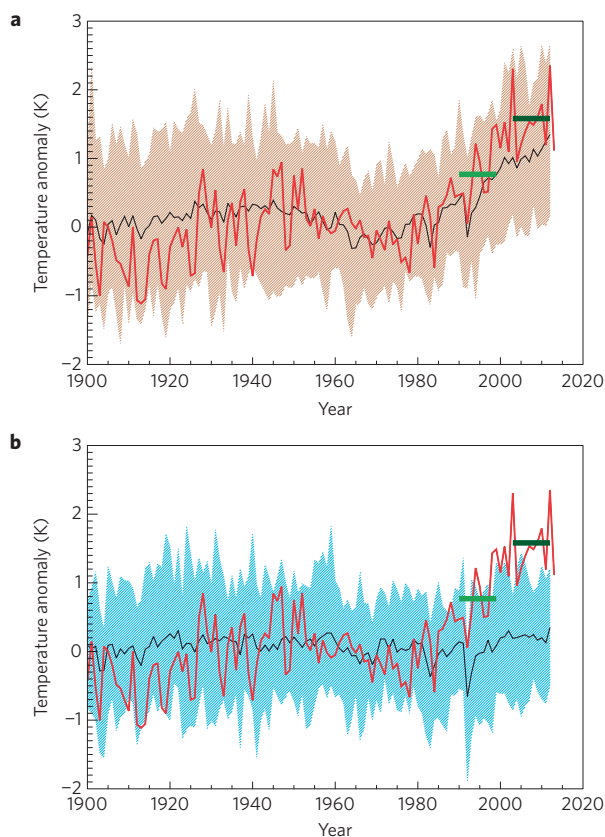
Met Office Hadley Centre, FitzRoy Road, Exeter EX1 3PB, UK. *e-mail: nikos.christidis@metoffice.gov.uk

**Figure 1 | Time series of the summer mean temperature anomaly relative to 1961–1990 in region 10° W–40° E, 30°–50° N.** Observed time series (red line) and the range of temperature anomalies from simulations with the seven CMIP5 models used in the analysis that include all forcings (red area, **a**), and from simulations that include natural forcings alone (blue area, **b**). The black line represents the time series of the mean of the model simulations. The observed mean anomalies in decades 1990–1999 (0.77 K) and 2003–2012 (1.58 K) are marked by the green horizontal lines.



**Figure 2 | Results from the optimal fingerprinting analyses. a,b,** Scaling factors for the 1920–1999 analysis (**a**) and the 1923–2012 analysis (**b**). The ellipse marks the two-dimensional 90th percentiles and the horizontal and vertical bars mark the 5–95% confidence interval for each of the two signals. Scaling factors corresponding to the climate response to anthropogenic and natural forcings are denoted by beta ANTHRO and beta NAT respectively. **c,** Normalized distributions of the regional summer mean temperature in decades 1990–1999 (dashed lines) and 2003–2012 (solid lines) including the influence of all external forcings (red) and natural forcings alone (blue). The vertical lines correspond to the two threshold used to define summer heatwaves. Temperature anomalies are relative to period 1961–1990. The plotted distributions were constructed with the data samples from optimal fingerprinting, binned and smoothed with running means for illustration purposes.

Scaling factors and their 5–95% uncertainty range are illustrated in Fig. 2a,b. In both analyses the anthropogenic signal can be detected in the observations, whereas the weaker natural signal is not detectable. The uncertainty in the scaling factors decreases when more recent years are included in the analysis, as the effect of human influence intensifies. However, the models tend to underestimate the anthropogenic response, which needs to be scaled up to best match the observations in the analysis extended to more recent years (scaling factors greater than unity). We derive observationally constrained estimates of the climate response with and without human influence in the 1990s and in 2003–2012 by extracting the last decade of the scaled time series we get from the optimal fingerprinting analyses. These estimates are then combined with unforced year-to-year temperature variations from control simulations to construct distributions of the regional summer temperature with and without the anthropogenic effect (Fig. 2c).

Whereas the summer temperature distribution in a hypothetical climate uninfluenced by human activity remains largely unchanged since the late twentieth century, in the actual climate regional warming associated with anthropogenic forcings is found to have led to a notable shift in the temperature distribution. As a result, the temperature anomaly threshold of 1.6 K, previously used to define a summer heatwave in the region[6], has moved from the warm tail to a more central sector of the temperature distribution in the past 10–15 years (Fig. 2c), suggesting a marked increase in the likelihood of extreme events. The more extreme anomaly of 2.3 K observed
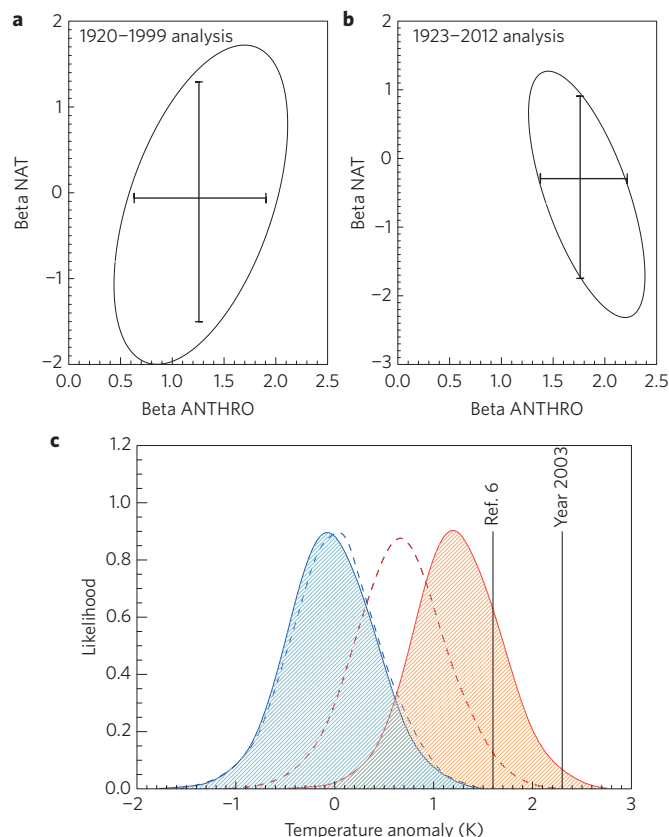
in the summer of 2003 lies outside the expected temperature distribution for the time the event occurred and even further away from the distribution of the natural climate. This suggests that although anthropogenic influence increased the chances of the event, it would still be considered a very rare one in 2003. On the other hand, the temperature distribution expected in the present day encompasses the 2.3 K threshold, which now lies in its warm tail. Hence, the additional shift of the distribution since 2003 means that although summers as warm as 2003 are still rare, they are now much more likely to occur.

We quantify the return time of extremely warm summers in the early 2000s and in the present day (approximated by decades 1990–1999 and 2003–2012 respectively), with and without anthropogenic effect, using the temperature distributions from our analysis. Uncertainties are also estimated using a bootstrap resampling technique (Methods) and the results are summarized in Table 1. Using the original threshold of 1.6 K we find a tenfold decrease in the return time of very hot summers from 52 years to 5 years (best estimates). When the effect of human influence is not accounted for, the likelihood of exceeding the threshold is
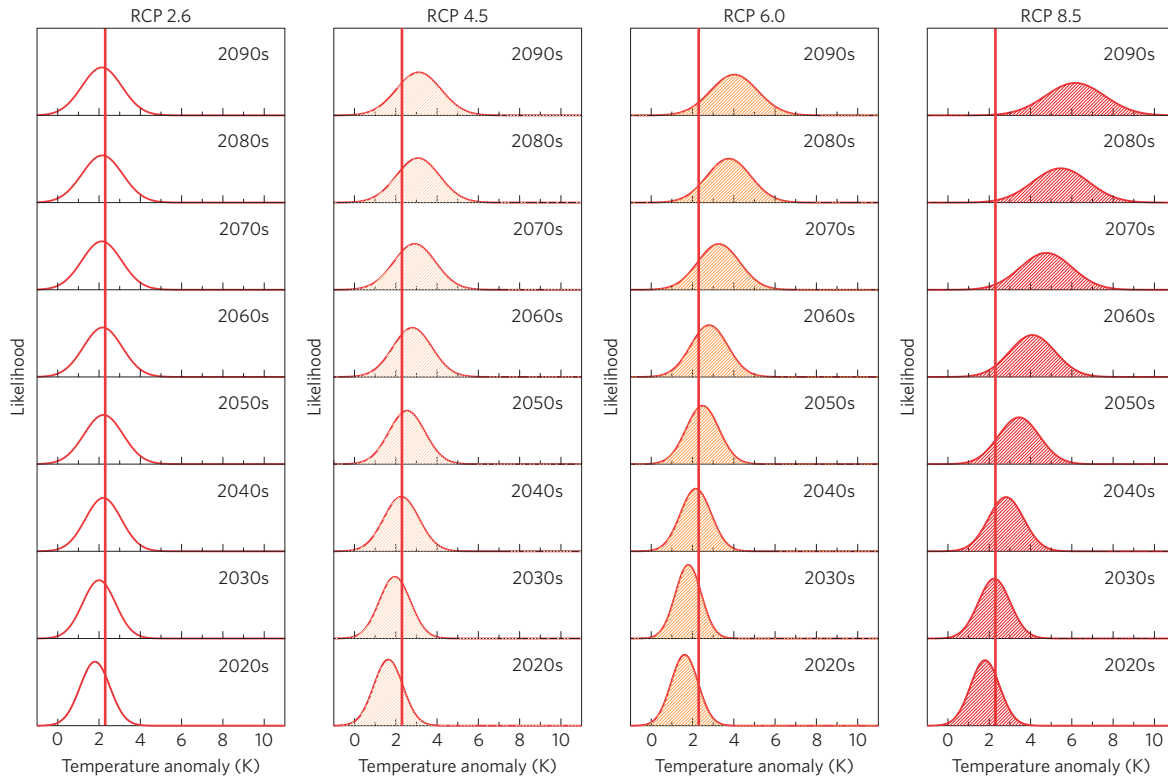
**Figure 3 | Normalized distributions of the summer mean temperature anomaly in future decades.** The distributions are constructed with data from all CMIP5 models that provided simulations with different RCPs. The RCP scenario is shown at the top of each vertical column of panels. Each distribution corresponds to the decade marked on its panel. Temperature anomalies are relative to period 1961–1990. The vertical line marks the temperature anomaly in summer 2003.

very small and although a much larger sample would be required to accurately estimate the likelihood, we get a clear indication that the return time is at least of the order of thousands of years. Hence, we find that the anthropogenic impact on the chances of the 2003 event is much greater than the doubling reported as a conservative estimate in the original study[6]. A possible reason for this discrepancy is that we now employ an ensemble of models rather than a single model in our fingerprinting analysis, which yields a smaller uncertainty in the scaling factors and therefore a smaller uncertainty in the warming attributed to different forcings. This leads to narrower temperature distributions and as a result the threshold lies further away into the warm tail of the distribution of the climate without the anthropogenic effect and the likelihood of exceeding the threshold is thus reduced.

We also estimate the return time of a summer as hot as in 2003 using the observed temperature anomaly of 2.3 K as a threshold. The likelihood of exceeding the threshold has sharply increased since the time of the event and conversely its return time has decreased from thousands of years to tens or hundreds of years (best estimate of 127 years). Given the current levels of climate change, an extremely hot summer in the reference region such as the one in 2003 would therefore be expected to occur about once a century. However, as climate warming continues, the distribution of the summer temperature is also expected to continue to move to warmer regimes, which would further increase the frequency of extreme events.

We use a cohort of model simulations (Supplementary Information) to examine how the summer temperature distribution in the reference region may change in future decades. We make use of all available data from experiments with CMIP5 models conducted with four different representative concentration pathways (RCPs), named after the value of the radiative forcing (in watts per square metre) in year 2100 (ref. 25). Here we use modelled temperatures without any scaling from optimal fingerprinting. For every RCP we

**Table 1 | Return times (RT) of summer heatwave events in the reference region, characterized by temperature anomalies above a given threshold and estimated with and without the effect of human influence on the climate (ALL and NAT).**

|  | Decade 1990–1999 | Decade 2003–2012 |
|---|---|---|
|  | Threshold = 1.6 K | |
| $RT_{ALL}$ (years) | 52 (14–444) | 5 (2.7–11) |
| $RT_{NAT}$ (years) | >$10^4$ | >$10^3$ |
| $PRB_{ALL}/PRB_{NAT}$ | >$10^3$ | >$10^3$ |
|  | Threshold = 2.3 K | |
| $RT_{ALL}$ (years) | >$10^3$ | 127 (34–999) |

The change in the probability due to anthropogenic forcings ($PRB_{ALL}/PRB_{NAT}$) is also shown for the 1.6 K threshold. Estimates in brackets correspond to the 5–95% uncertainty range. For probabilities too small to be accurately estimated, a best approximation of the order of magnitude of the 5th percentile is reported.

fit a normal distribution to the model data using all the years in each decade from the 2020s to the 2090s (Fig. 3). It should be noted that the normal distribution is used here as a simple illustration of future changes in temperature. Probabilities of events need to employ distributions that represent better the overall shape and tails of the distribution, as indeed done in our study (Methods). Apart from RCP2.6, we find an evident shift of the temperature distribution with time towards warmer values. All RCPs indicate that by the 2040s a summer as hot as 2003 will be very common, and RCPs with the strongest anthropogenic influence (RCP6.0 and RCP8.5) suggest the 2003 summer will be deemed an lextremely cold event by the end of the century. These results are in agreement with earlier model projections made in the aftermath of the 2003 event[6].

Anthropogenic influence on the climate may have strongly regulated the frequency of extremely hot European summers in the past 10–15 years according to our study. With summer temperatures on an upward trajectory, the perception of extremely hot summers in Europe is set to change markedly over the next few decades. Increasing society's resilience to heatwaves in the region is therefore highlighted as a critical challenge that adaptation planners need to consider. To this end the recent launch of the EUropean CLimate and weather Events: Interpretation and Attribution (EUCLEIA) project[26] aims to provide decision-makers with timely and reliable assessments on how extreme weather and climate risk in Europe is changing owing to human influence.

## Methods

**Optimal fingerprinting.** Decadal summer temperatures averaged over the reference region in consecutive decades during the analysis period are estimated with data from CRUTEM4 and simulations with ALL and NAT forcings. Temperatures are expressed as anomalies relative to the 1961–1990 base period, that is, the same as in the CRUTEM4 data set. Using an earlier base period to approximate the pre-industrial climate was found to introduce uncertainty in the results without, however, changing the main conclusions of our study (Supplementary Information). The model data are first masked by the observations to include the same spatial coverage. For each experiment (ALL and NAT) we take the mean of all available simulations for each model and then compute the average of the ensemble means of the seven models used in the analysis[23]. The temperature time series constructed from this multi-model ensemble are organized into vectors $\mathbf{x}_{ALL}$ and $\mathbf{x}_{NAT}$ and the observational time series is similarly organized into a vector $\mathbf{y}$. The anthropogenic response, $\mathbf{x}_{ANT}$, is approximated by the difference $\mathbf{x}_{ALL} - \mathbf{x}_{NAT}$. Optimal fingerprinting decomposes the observations into the forced response and unforced variability:

$$\mathbf{y} = (\mathbf{x}_{ANT} - \mathbf{u}_{ANT})\beta_{ANT} + (\mathbf{x}_{NAT} - \mathbf{u}_{NAT})\beta_{NAT} + \mathbf{u}_0$$

The effect of internal variability in the observations and the simulated response is represented by the noise terms $\mathbf{u}_0$, $\mathbf{u}_{ANT}$ and $\mathbf{u}_{NAT}$. We carry out two analyses: the first covers the period 1920–1999 as in a previous study of the 2003 heatwave[6] (that is, uses decadal temperature anomalies in eight consecutive decades 1920–1929, …, 1990–1999); the second spans years 1923–2012 (that is, uses anomalies in decades 1923–1932, …, 2003–2012). The variance–covariance matrix of the noise terms is derived from independent segments of equal length to the analysis period extracted from the control simulations of the unforced climate, processed and organized into vectors ($\mathbf{Y}$) in the same way as the observations:

$$\mathbf{C}_N = \frac{1}{n}\mathbf{Y}_N\mathbf{Y}_N^T$$

where $n$ denotes the number of control segments and $N$ the vector length. We use 75 segments for the 1920–1999 analysis and 68 segments for the 1923–2012 analysis. The control simulations are also used to estimate the uncertainty in the scaling factors and test whether the modelled internal variability and the regression residuals are consistent[22], which is indeed found to be the case in our study. As common in optimal fingerprinting, the analysis is carried out in a transformed space defined by the leading empirical orthogonal functions of the internal variability estimated from the control segments. We retain the seven leading empirical orthogonal functions, which explain more than 90% of the observed variability. Each analysis outputs the best estimate and the 5–95% uncertainty range of the $\beta_{ANT}$ and $\beta_{NAT}$ scaling factors. A signal is detectable, if the uncertainty range of the corresponding scaling factor does not encompass zero.

**Temperature distributions and the likelihood of a threshold exceedance.**
Optimal fingerprinting provides observationally constrained estimates of the response to anthropogenic and natural forcings, as well as the response to all forcings (from the linear combination ANT+NAT). Our fingerprinting algorithm yields $10^5$ possible estimates of each scaling factor (by sampling each percentile of the distribution 1,000 times) representing the uncertainty in their value, from which we get $10^5$ estimates of the temperature change in the reference region attributed to different forcings. By extracting the last decade we obtain samples of the climate response to all and natural forcings in the 1990s (from the 1920–1999 analysis) and the most recent decade of 2003–2012 (from the 1923–2012 analysis). We then combine these response estimates with a sample of ∼3,500 summer temperature anomalies of individual years in non-overlapping decades from control experiments (representing the effect of internal variability) and construct the temperature distributions with and without the effect of human influence in the early 2000s and the present-day (Fig. 2c).

The probability of warm summers and the associated uncertainty are estimated as follows: we add each of the $10^5$ estimates of the forced decadal temperature response to all the annual temperature estimates for the unforced climate and compute $10^5$ estimates of the probability of exceeding a threshold using order statistics, or, the generalized Pareto distribution, if the threshold lies in the tail of the distribution. The resulting sample provides the 50th percentile (best estimate) and the 5th and 95th percentiles of the probability of an extreme event (that is, regional summer temperature above the threshold). The return time is computed as the inverse of the probability. When the threshold lies in the far tail of the temperature distribution, the probability estimates are very small and the corresponding return times are of the order of a thousand years or more (based on the 5th percentile). The precise return time of these extremely rare events cannot be reliably estimated because of the insufficient sample size and we report only a conservative estimate of the order of magnitude of the return time.

## References

1. Bindoff, N. L. *et al.* in *Climate Change 2013: The Physical Science Basis* (eds Stocker, T. *et al.*) 867–952 (IPCC, Cambridge Univ. Press, 2013).
2. Stott, P. A. *et al.* in *Climate Science for Serving Society: Research, Modeling and Prediction Priorities* (eds Asrar, G. R. & Hurrell, J. W.) (Springer Science + Business Media, 2013).
3. Schär, C. *et al.* The role of increasing temperature variability in European summer heatwaves. *Nature* **427,** 332–336 (2004).
4. Beniston, M. The 2003 heat wave in Europe: A shape of things to come? An analysis based on Swiss climatological data and model simulations. *Geophys. Res. Lett.* **31,** L02202 (2004).
5. Robine, J-M. *et al.* Death toll exceeded 70,000 in Europe during the summer of 2003. *C. R. Biol.* **331,** 171–178 (2008).
6. Stott, P. A., Stone, D. A. & Allen, M. R. Human contribution to the European heatwave of 2003. *Nature* **432,** 610–613 (2004).
7. Meehl, G. A. *et al.* Model-based evidence of deep-ocean heat uptake during surface-temperature hiatus periods. *Nature Clim. Change* **1,** 360–364 (2011).
8. Fyfe, J. C., Gillett, N. P. & Zwiers, F. W. Overestimated global warming over the past 20 years. *Nature Clim. Change* **3,** 767–769 (2013).
9. Kosaka, Y. & Xie, S. Recent global-warming hiatus tied to equatorial Pacific surface cooling. *Nature* **501,** 403–407 (2013).
10. Seneviratne, S. I., Donat, M. G., Mueller, B. & Alexander, L. V. No pause in the increase of hot temperature extremes. *Nature Clim. Change* **4,** 161–163 (2013).
11. Sillmann, J., Donat, M. G., Fyfe, J. C. & Zwiers, F. W. Observed and simulated temperature extremes during the recent warming hiatus. *Environ. Res. Lett.* **9,** 064023 (2014).
12. Dole, R. *et al.* Was there a basis for anticipating the 2010 Russian heat wave? *Geophys. Res. Lett.* **38,** L06702 (2011).
13. Rahmstorf, S. & Coumou, D. Increase of extreme events in a warming world. *Proc. Natl Acad. Sci. USA* **108,** 17905–17909 (2011).
14. Luo, L. & Zhang, Y. Did we see the 2011 summer heat wave coming? *Geophys. Res. Lett.* **39,** L09708 (2012).
15. Lewis, S. & Karoly, D. J. Anthropogenic contributions to Australia's record summer temperatures of 2013. *Geophys. Res. Lett.* **40,** 3705–3709 (2013).
16. Peterson, T. C., Stott, P. A. & Herring, S. Explaining extreme events of 2011 from a climate perspective. *Bull. Am. Meteorol. Soc.* **93,** 1041–1067 (2012).
17. Peterson, T. C., Hoerling, M. P., Stott, P. A. & Herring, S. Explaining extreme events of 2012 from a climate perspective. *Bull. Am. Meteorol. Soc.* **94,** S1–S74 (2013).
18. Herring, S. C., Hoerling, M. P., Peterson, T. C. & Stott, P. A. Explaining extreme events of 2013 from a climate perspective. *Bull. Am. Meteorol. Soc.* **95,** S1–S96 (2014).
19. Giorgi, F. & Francisco, R. Uncertainties in regional climate change prediction: A regional analysis of ensemble simulations with the HADCM2 coupled AOGCM. *Clim. Dynam.* **16,** 169–182 (2000).
20. Jones, P. D. *et al.* Hemispheric and large-scale land surface air temperature variations: An extensive revision and an update to 2010. *J. Geophys. Res.* **117,** D05127 (2012).
21. Taylor, K., Stouffer, R. J. & Meehl, G. A. An overview of CMIP5 and the experimental design. *Bull. Am. Meteorol. Soc.* **93,** 485–498 (2012).
22. Allen, M. R. & Stott, P. A. Estimating signal amplitudes in optimal fingerprinting, part I: Theory. *Clim. Dynam.* **21,** 477–491 (2003).
23. Jones, G. S., Stott, P. A. & Christidis, N. Attribution of observed historical near surface temperature variations to anthropogenic and natural causes using CMIP5 simulations. *J. Geophys. Res.* **118,** 4001–4024 (2013).

24. Christidis, N., Stott, P. A. & Zwiers, F. W. Fast-track attribution assessments based on pre-computed estimates of changes in the odds of warm extremes. *Clim. Dynam.* http://dx.doi.org/10.1007/s00382-014-2408-x (2014).
25. Moss, R. H. *et al.* The next generation of scenarios for climate change research and assessment. *Nature* **463,** 747–756 (2010).
26. http://eucleia.eu/

## Acknowledgements

## Author contributions

N.C. organized the research, performed the analysis and wrote the paper. G.S.J. provided comments and data for the analysis. P.A.S. provided comments and contributed to the text.

## Additional information

Supplementary information is available in the online version of the paper. Reprints and permissions information is available online at www.nature.com/reprints. Correspondence and requests for materials should be addressed to N.C.

## Competing financial interests

The authors declare no competing financial interests.